Article

Not peer-reviewed version

Study on the mechanical property and design method of frame-unit bamboo culm members based on semi-rigid joints

Guojin Wang , Xin Zhuo * , Shenbin Zhang , Jie Wu

Posted Date: 7 March 2024

doi: 10.20944/preprints202403.0387.v1

Keywords: frame-unit prefabricated bamboo culm structure; semi-rigid joint; mechanical property; numerical simulation methods; design method.

Article

Study on the Mechanical Property and Design Method of Frame-Unit Bamboo Culm Members Based on Semi-Rigid Joints

Guojin Wang [1,3], Xin Zhuo [2,3,*], Shenbin Zhang [2] and Jie Wu [2]

1 Center for Balance Architecture, Zhejiang University, Hangzhou 310028, China
2 Architectural Design & Research Institute of Zhejiang University Co., Ltd, Hangzhou 310028, China
3 Department of Civil Engineering, Zhejiang University, Hangzhou 310058, China
* Correspondence: Author: Xin Zhuo. Email: zhuoxin@zju.edu.cn

Abstract: This paper proposes a lightweight joint with bamboo culm cross connection, which is constructed by screwing one side of the screw into the other side of the wooden plug, its simple construction makes it easy to manufacture and cost-effective. This form connects adjacent bamboo culms to form corner joints, and bolt connects adjacent bamboo culm frames to form edge joints, to explore the mechanical properties of the combination joints formed by corner joints and edge joints, by combining experiments and numerical simulations, the method discovered and explained the relationship and mechanism between the number and position of bolts and the stiffness of edge joints. A calculation model for frame-unit bamboo culm members considering semi-stiffness of joints is proposed, and the conversion equations between linear stiffness of corner and edge joint and their rotational stiffnesses are derived. By establishing the series and parallel relationship between the corner and edge joints in the assembled members, a generalized relational equation between the total stiffness of the assembled joint and the stiffness of the corner and edge joints is derived. A numerical simulation method for frame-unit bamboo culm members with semi-rigid joints is proposed, which can obtain the stiffness calculation formula of edge joints and the average rotational stiffness value of semi-rigid corner joints. A finite element analysis method based on semi-rigid joints is proposed for frame-unit bamboo culm members, and the internal force sketches and calculation methods for bamboo culms and joints are presented, which can be used for the internal force analysis and design of frame-unit bamboo culm lattice structures.

Keywords: frame-unit prefabricated bamboo culm structure; semi-rigid joint; mechanical property; numerical simulation methods; design method

1. Introduction

The production process of building materials such as steel bars and cement generates a large amount of carbon and harmful gas emissions [1], exacerbating global climate issues such as climate change and environmental pollution, promoting natural building materials can help alleviate these problems. Bamboo and wood are two common natural building materials that have been widely used in construction projects, where bamboo has higher carbon sequestration efficiency [1] and better mechanical properties than wood [2, 3]. A series of studies and engineering examples have proved the feasibility of bamboo as a building material [4, 5]. Compared with engineered bamboo, raw bamboo culms do not require the use of adhesives and are more environmentally friendly as a building material.

The different cross-sectional geometries of natural bamboo culms, the anisotropy of bamboo materials, the different mechanical properties of different parts of the same bamboo culm [6], and the different orientations of different joints connecting different bamboo tubes in the bamboo tube

Preprints.org (www.preprints.org) | NOT PEER-REVIEWED | Posted: 7 March 2024 doi:10.20944/preprints202403.0387.v1

structure constrain the standardization of the design of the bamboo tube structures and bring difficulties to the promotion of the bamboo tube structure. Hong et al. [7] divided the common bamboo tube connection joints into two categories of traditional joints and modern joints, where the traditional joints include tied connections and mortise and tenon connections, and the modern joints include types such as bolts, steel components, and fillers. In the German-Chinese House at the Shanghai World Expo 2010 [8], the joints are made of steel prefabricated parts with grouting, and the prefabricated steel components are capable of connecting bamboo tubes in different directions. Huang et al. [9] proposed a bamboo tube joint using grouting and built-in steel sheet connection, and the tests showed that this type of joint has high load bearing capacity. The above improved grouted joints showed better mechanical properties, but the grouting would significantly increase the self-weight of the structure and could not take advantage of the light weight of the bamboo tube structure. Richard et al. [10] proposed a new type of joint connecting bamboo tubes with steel rings and pieces, and the stiffness and strength of this type of joint were proved to be more than that of the traditional grouted bamboo tube joint through tests. Benoit et al. [11] proposed a bamboo tube joint using a combination of wood plugs and metal clamps, and demonstrated through experiments and numerical simulations that the joint can be used for the longitudinal extension of bamboo tubes with good strength, providing a new idea for lightweight joints of bamboo tube structures. In this paper, a lightweight joint for cross connection of bamboo tubes is proposed as shown in Figure 1a, where wood plugs are embedded in each of the two sides of the bamboo tubes, and each screw is screwed from the outside of one side of the bamboo tube into the wood plug inside the other side of the bamboo tube, and the bamboo tube and the wood plugs are cut at the same angle in the joint part. The joint has the advantages of light weight, easy production, and low cost.

The existing bamboo tube space structures can be divided into two types: [12, 13] bamboo tube arch structure and bamboo tube lattice structure. Bend and connect one or more long bamboo tubes to form a large-span bamboo tube arch structure, the disadvantage is that the bending process using manual labor makes it difficult to control processing accuracy. The bamboo tube lattice structure uses straight bamboo tubes, which are easy to process and low in cost, but the processing difficulty of multi-directional joints and the customization cost is high. Zhuo et al. [14, 15] proposed a framed bamboo culm grid structure system(Frame-unit prefabricated bamboo culm structure), the formation principle is shown in Figures 1c and 1d: straight bamboo culms are assembled into bamboo culm frame units, which can be in polygonal geometries such as triangles, rectangles, trapezoids, hexagons, and other polygonal geometries; the joints of neighboring culms are called corner joints, which can be connected by a combination of grouting, screws, and wood plugs (Figure 1a); and the joints between neighboring bamboo culm frames are called edge joints, which use bolts as connectors (Figure 1b).

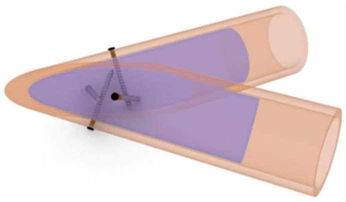

(a) Corner joint

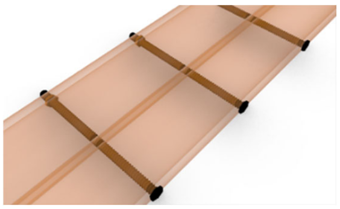

(b) Edge joint

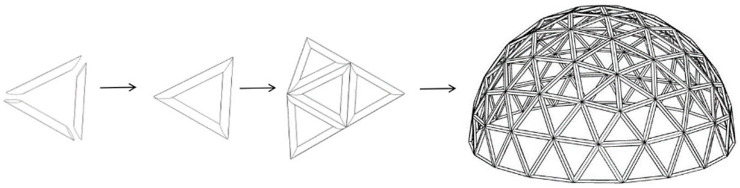

(c) Formation of structure

Preprints.org (www.preprints.org) | NOT PEER-REVIEWED | Posted: 7 March 2024 doi:10.20944/preprints202403.0387.v1

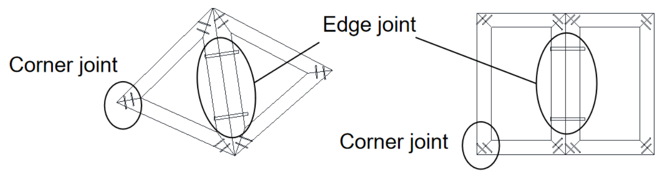

(d) The Corner joint and Edge joint

Figure 1. Structural forming principles and two types of joints.

After all the bamboo culm frame units are connected, the overall structure can be formed. This paper employs experimental, numerical simulation, and theoretical analysis to investigate the flexural performance of frame-unit bamboo culm joints. The focus is on studying the semi-rigid bearing mechanism and calculation method for joints when materials are in the elastic phase at edge and corner joints

2. Bamboo Culm Frame Specimen Bending Performance Test

2.1. Overview of the Test

In this paper, the specimens were assembled by two neighboring rectangular bamboo culm frames connected by bolts (Figure 2a), with the diameter of the bamboo culms ranging from 75 mm to 95 mm and the wall thickness ranging from 7.5 mm to 8.5 mm. The corner joints of the bamboo culm frames were embedded with wood plugs inside and were connected using four 4mm diameter screws (Figure 2b). The edge joints are made of Q235 bolts with a diameter of 10 mm and a length of about 200 mm.

(a) Edge joint **(b)** Corner joint

Figure 2. Corner joint and Edge joint.

The specimens were rested in a simply supported manner on the bull legs of the steel frame test rig (shown in Figure 3).

Preprints.org (www.preprints.org) | NOT PEER-REVIEWED | Posted: 7 March 2024 doi:10.20944/preprints202403.0387.v1

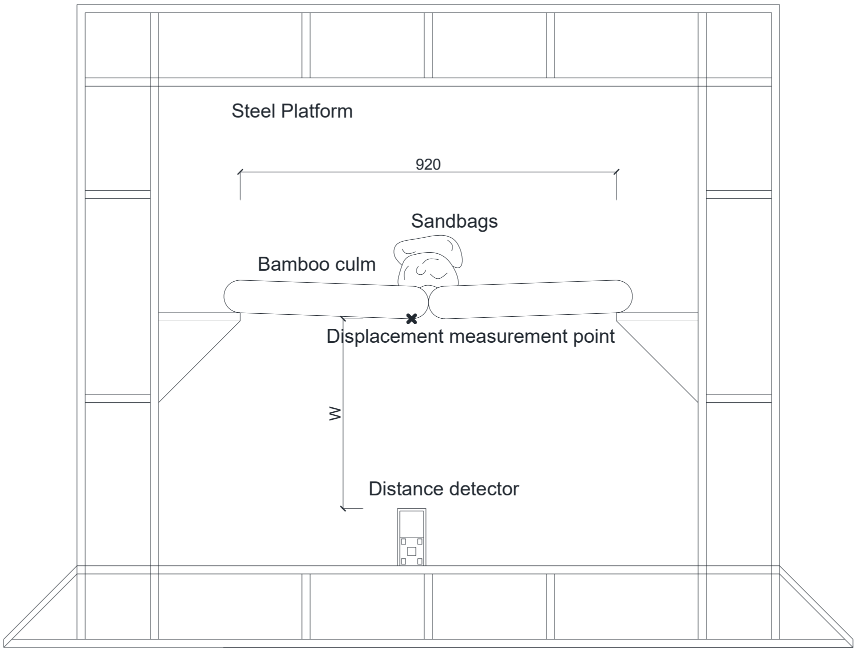

Figure 3. Loading device.

The positions of bolt holes are marked as A, B, C, B′, A′ respectively. The dimensions of the assembled specimens are shown in Figure 4. Loading tests were conducted on specimens with 2, 3, and 5 bolts connected to the edge joints, the experimental parameters for each model are shown in Table 1 The specimen number “Sn” indicates that the number of bolts in the edge joint is n.

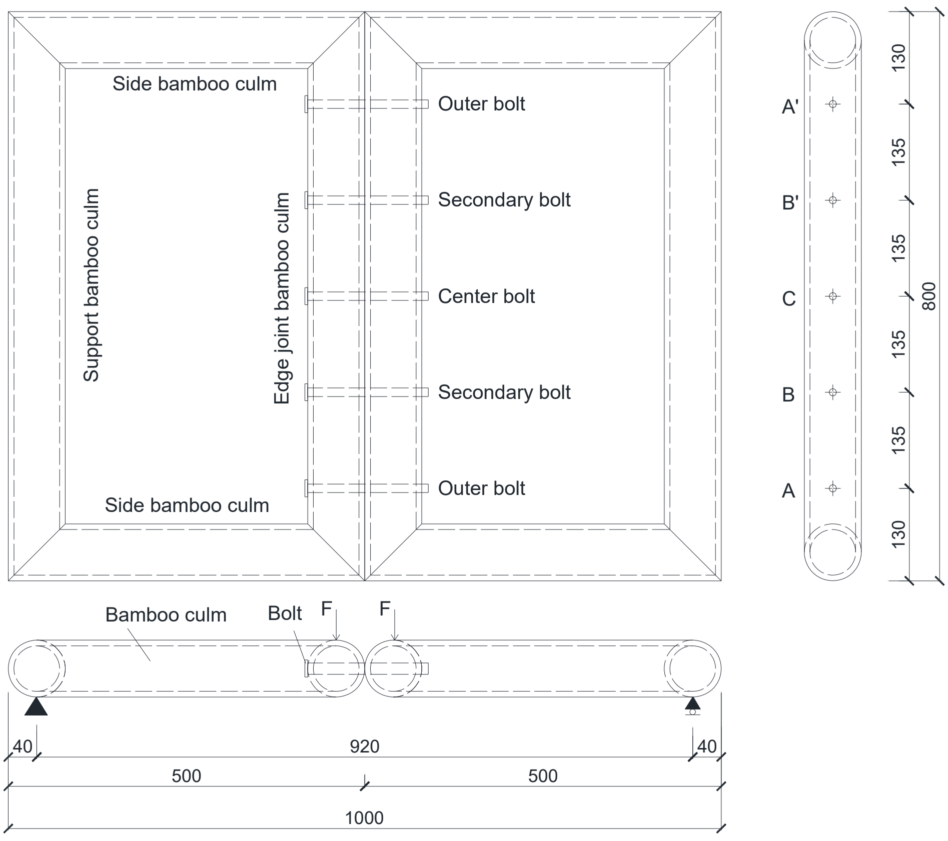

Figure 4. Dimensions of specimens (unit: mm).

Preprints.org (www.preprints.org) | NOT PEER-REVIEWED | Posted: 7 March 2024 doi:10.20944/preprints202403.0387.v1

Table 1. Test variable.

Specimens number	$S2_{test}$	$S3_{test}$	$S5_{test}$
Bolt positions	A, A′	A, C, A′	A, B, C, B′, A′
Maximum load applied (N)	620.3	620.3	620.3

2.2. Experimental Process and Result Analysis.

The two bamboo culm frames of the specimen are in the same plane when unloaded. Loading is done by stacking sandbags, with each sandbag weighing 10kg (±0.5kg). The loading position is in the middle of the specimen (Figure 3). Vertical displacement occurs at the edge joint positions of the specimen, gradually increasing with the number of sandbags (Figure 5a), and there's a gap between the two bamboo culms at the corner joint (Figure 5b). The measuring point for vertical displacement is at the midpoint of the lower edge of the edge joint bamboo culm (Figure 3), measured using a laser distance detector with an accuracy of 0.1mm. During loading, sandbags are placed one by one, and data from the displacement detector is read only after the vertical displacement stabilizes after placing a sandbag (the unloading stage is similar). The deflection of the measuring point under each stage of loading is:

$$u_i = w_i - w_0 \tag{1}$$

where w_i is the reading at stage i, and w_0 is the reading without load. The data recorded at each loading step is used to create the load-displacement relationship shown in Figure 6.

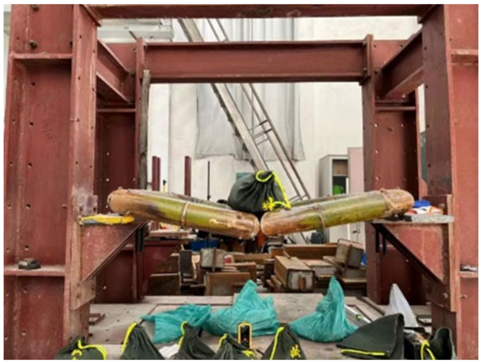

(a) Edge joint deformation

(b) Corner joint deformation

Figure 5. Deformation of test specimen joints after loading.

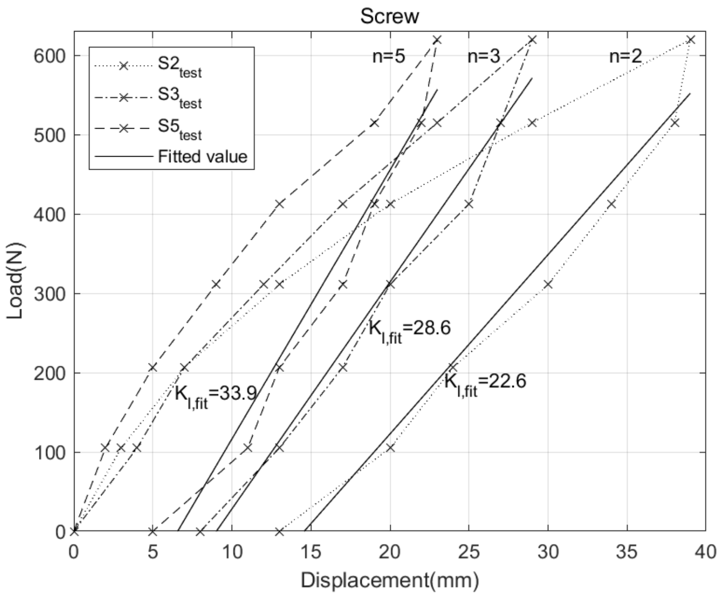

 doi:10.20944/preprints202403.0387.v1

Figure 6. Experimental data and fitted values.

Before loading, due to the presence of bamboo nodes, it is impossible to achieve complete fit between the outer walls of adjacent bamboo culms. In addition, it is also impossible to achieve a complete fit between the bamboo culm bolt hole wall and the bolt thread, so the deformation during the loading process includes measurement errors caused by these factors. In contrast, the unloading process has achieved close contact between different materials, and the corresponding load-displacement relationship can better reflect the true mechanical properties of the specimens.

The total bending linear stiffness K_l (hereafter referred to as total linear stiffness) of the bamboo culm frame in the elastic phase is defined as the ratio of the out-of-plane load at the edge joints to the vertical displacement occurring in the direction of action:

$$K_l = \frac{\Delta F}{\Delta d} \tag{2}$$

where ΔF and Δd are the incremental load and displacement of the measuring point.

The test data from the unloading stage were selected for linear fitting (using the polyfit function in MATLAB) to obtain the fitted values of total linear stiffness $K_{l,fit}$ (Figure 6), which shows that the total bending linear stiffness is positively correlated with the number of bolts. However, as the number of bolts increases, the efficiency of stiffness increases decreases gradually.

2.3. Synergistic Relationship between Corner Joints and Edge Joints.

During the loading process, no visible bending occurred in each bamboo culm, while vertical displacement occurred at the edge joints. At the same time, the gap at the corner joints gradually widened with the increase of the load (Figure 5b), indicating that the corner joints and edge joints are not completely rigid (semi-rigid). Define k_{sa} and k_{ca} as the rotational stiffness of the edge joints and corner joints, respectively:

$$k_{\text{sa}} \overset{\text{def}}{=} \frac{\Delta M_{\text{s}}}{\Delta \theta_s} \tag{3}$$

$$k_{\text{ca}} \overset{\text{def}}{=} \frac{\Delta M_{\text{c}}}{\Delta \theta_c} \tag{4}$$

where M_s, θ_s are the bending moments and turning angles of the edge joints, M_c, θ_c are the bending moments and turning angles of the corner joints, and the units of bending moments and turning angles are $N \cdot mm, Rad$, respectively.

To convert the relationship between force and displacement into the relationship between bending moment and rotation, the various bamboo culms are simplified into rigid members, and a simplified diagram for the internal force calculation of the frame-unit bamboo culm members shown in Figure 7 is established.

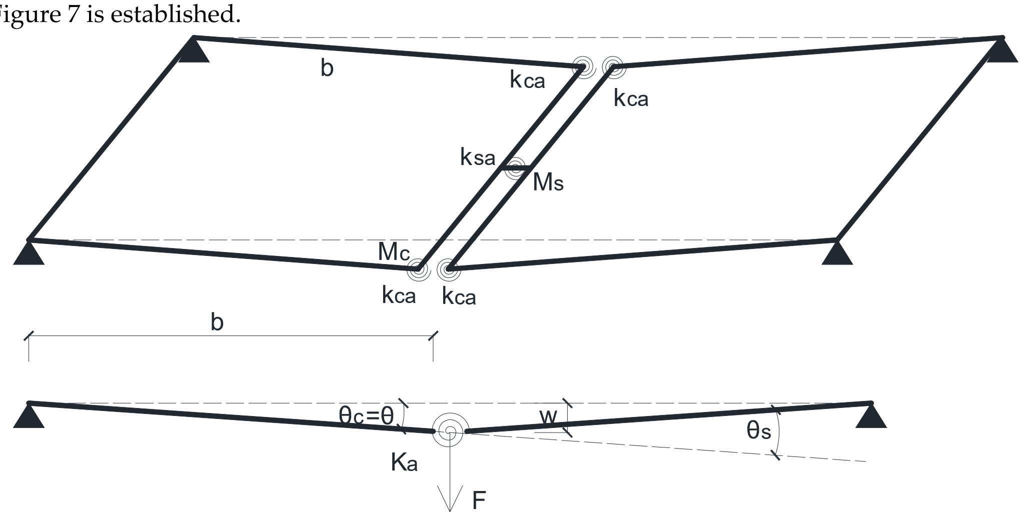

 doi:10.20944/preprints202403.0387.v1

Figure 7. Schematic diagram for structural deformation calculation.

In Figure 7, F is the vertical force acting on the upper surface of the edge joint bamboo culm. Under the action of F, both the edge joint and the corner joints produce vertical displacement.

When the corner joints are completely rigid, define the edge joint linear stiffness:

$$k_{\mathrm{sl}} \overset{\mathrm{def}}{=} \frac{\Delta F}{\Delta w} \tag{5}$$

When the edge joint is completely rigid, define the corner joint linear stiffness:

$$k_{\mathrm{cl}} \overset{\mathrm{def}}{=} \frac{\Delta F}{\Delta w} \tag{6}$$

According to Figure 7:

$$\begin{cases} M_s = 0.5Fb \\ \theta_s = 2\theta \end{cases} \tag{7}$$

$$\begin{cases} M_c = 0.25Fb \\ \theta_c = \theta \end{cases} \tag{8}$$

where: b is the distance between the axis of edge joint bamboo culm and support bamboo culm (hereinafter referred to as the shear span). When the structural deformation is small:

$$\theta \sim \tan\theta = \frac{w}{b} \tag{9}$$

The numerator and denominator in equation 3 are represented by ΔF and Δw respectively, the relationship between the edge joint linear stiffness and its rotational stiffness can be obtained:

$$k_{sa} = \frac{0.5\Delta Fb}{2\Delta\theta} = \frac{0.5\Delta Fb}{2\frac{\Delta w}{b}} = \frac{b^2}{4}k_{sl} \tag{10}$$

Similarly, the relationship between the corner joint linear stiffness and its rotational stiffness can be obtained from equation 4:

$$k_{ca} = \frac{b^2}{4}k_{cl} \tag{11}$$

The unit of edge and corner joint linear stiffness is N/mm. From equations 5 and 6, the linear stiffness is not a property of the joint itself, and its value is related to structural parameters such as rotational stiffness and span.

In structural mechanics, the shear distribution method is solved by analyzing the series-parallel relationship and stiffness relationship of the members [16]. In the structure shown in Figure 7, the two corner joints in a bamboo culm frame single-sided structure are in parallel relationship, and the relationship between the corner joints and the edge joint constitutes a series relationship, and the series and parallel relationships of the assembled joints are shown in Figure 8:

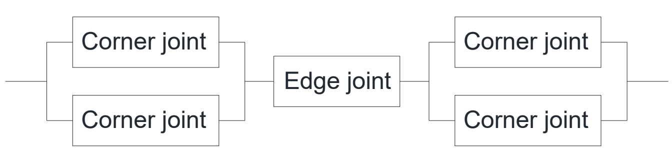

Figure 8. Series and parallel relationships between the joints.

According to Figure 8, establish the relationship between the overall rotational stiffness and that of the edge and corner joints.

$$\frac{1}{K_a} = \frac{1}{2k_{ca}} + \frac{1}{k_{sa}} + \frac{1}{2k_{ca}} = \frac{1}{k_{ca}} + \frac{1}{k_{sa}} \tag{12}$$

Preprints.org (www.preprints.org) | NOT PEER-REVIEWED | Posted: 7 March 2024 doi:10.20944/preprints202403.0387.v1

Similarly, the relationship between total linear stiffness and the linear stiffness of the edge and corner joints can be established:

$$\frac{1}{K_l} = \frac{1}{k_{cl}} + \frac{1}{k_{sl}} \tag{13}$$

3. Numerical Simulation

3.1. Overview

3.1.1. Setting of Numerical Simulation

1. The finite element software Abaqus is used for modelling and calculation of numerical simulation. Since the two neighboring bamboo culm frames have symmetry, in order to improve the computational efficiency, only a single bamboo culm frame is established, and symmetrical constraints are applied to the mid-span cross sections of truncated bolts;
2. The influence of bamboo nodes is not taken into account;
3. The actual bamboo culm wall has different elastic modulus along the axial, lateral and radial directions, which is simplified by setting up bamboo culms as orthotropy material in both axial and lateral directions, and ignoring the difference in the mechanical parameters of the bamboo culms along the radial direction;
4. The diameter of the opening of the bamboo culm is the same as the diameter of the bolt, which is taken as 10 mm, ignoring the effect of the thread on the bamboo culm;
5. The loading plate for applying load is set to simulate the sandbag load in the test.

3.1.2. Material Properties

According to the test data of García et al. [17], the mechanical properties of bamboo are shown in Table 2, where: direction 2 is the bamboo culm axis (fiber) direction, and directions 1 and 3 are perpendicular to the axis direction (the bamboo culm material property setting direction is the local coordinate system of the bamboo culm). E_{mn}, V_{mn}, and G_{mn} are the elastic modulus, Poisson's ratio, and shear modulus. The yield strength of the bolt is 235MPa, the elastic modulus is 206GPa, and the Poisson's ratio v is 0.3; according to the axial compression test conducted by Zhang et al. [18, 19], the axial compressive yield strength is 50.3Mpa, and the shear yield strength is 25Mpa. The compressive strength σ_c of the bamboo culm groove is calculated according to the formula proposed by Peng Hui et al. [20]:

$$F_s = 0.8\sigma_1 dt \tag{14}$$

where: F_s is the yield load of bearing compression of bolt hole, σ_1 is the compressive strength of bamboo culm with grain, d is the diameter of the hole, and t is the thickness of the bamboo culm. Rewrite equation 14, can get the compressive strength of bamboo culm at the location of the bolt hole wall:

$$\sigma_c = \frac{F_s}{dt} = 0.8\sigma_1 = 40.2MPa \tag{15}$$

Table 2. Properties of bamboo materials.

E_1	E_2	E_3	V_{23}	V_{13}	V_{12}	G_{23}	G_{13}	G_{12}
398	14700	398	0.3	0.14	0.008	581	175	581

3.1.3. Calculation Model

The friction coefficient between the bolt and the wall of the bamboo culm is set at 0.3; the normal direction is set as "hard contact", and only pressure is transmitted between them. The loading plate is set as a rigid body, The friction coefficient between its lower face and the bamboo culm is set at 0, loading plate transmits pressure only. (does not play the role of a member).

The model numbers and bolt positions of the numerical simulation are the same as Table 1. The outer diameter of the bamboo culm is 80mm, and the wall thickness is 8mm. The components include bamboo culms, and bolts (Figure 9), with the bamboo culms consisting of edge joint bamboo culm, support bamboo culm and side bamboo culms, all dimensions of the components are consistent with Figure 4. The support bamboo culm is set as a simply supported constraint, restricting the displacement in the y and z directions at various points on its lower edge, and constraining the displacement in the x direction at various points on the cross-section of the bolt midspan. The mesh type used is C3D8R. To be consistent with the experiment, the loading range of the edge joint bamboo culm does not include the beveled area at the end of the bamboo culm. A gradually increasing concentrated force is applied to the upper surface of the loading plate until one of the bolts yields.

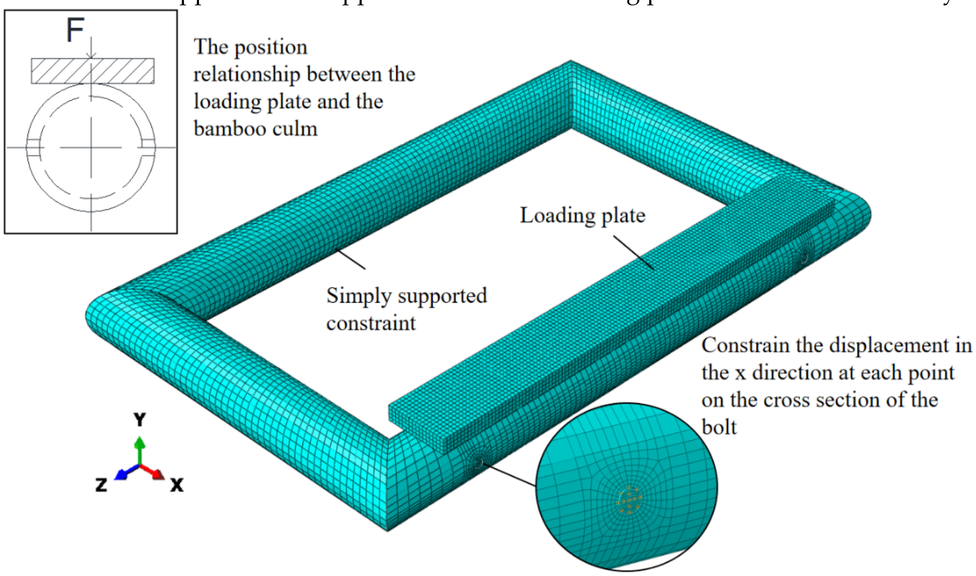

Figure 9. Loading surface and boundary conditions.

3.2. Semi-Rigid Corner Joint

Due to the complexity of the forces in the corner joint area of the bamboo culm frame, the corner joints in the numerical simulation will be modelled and calculated as full rigidity and semi-rigidity respectively.

3.2.1. Set the Corner Joint to Be Fully Rigid.

The end faces of the neighboring bamboo culms are set into coupling constraints, and the relative angle between the end faces of the side bamboo culms and the end faces of the edge joint bamboo culms is maintained at 0. To study the deformation of the structure when the materials are all in the elastic phase, extract the yield loads for each model from the post-processing module of the numerical simulation. When the loads were 245N, 330N and 460N respectively, the bolts of the models with the number of bolts at the edge joints of 2, 3 and 5 yielded respectively. Currently, no plastic deformation occurs at both bolt holes and bamboo culm walls. The cross-sections of each bolt span were subjected to bending moment around the Z-axis direction, and the proportion of the bending moment of each bolt is shown in Table 3.

Table 3. Bending moment ratio of each bolt.

Bolt position	n=2	n=3	n=5
A	0.5	0.366	0.258
B	/	/	0.169

Preprints.org (www.preprints.org) | NOT PEER-REVIEWED | Posted: 7 March 2024 doi:10.20944/preprints202403.0387.v1

C	/	0.268	0.146

The vertical displacements of the displacement measurement points corresponding to the experiment are recorded as w_{50} and w_{100} for 50N and 100N loads, respectively.

The total linear stiffness value $K_{l,sim}$ of the structure when the corner joint is fully rigid is calculated according to equation.16, and the fitted value $K_{l,fit}$ is obtained according to the test data, both of which are shown in Table 4, which shows that there is a big difference between numerical simulation and test values when the corner joint is set to be fully rigid, it is therefore necessary to change the setting of the corner joint to be semi-rigid.

$$K_{l,sim} = 2\frac{\Delta P}{\Delta w} = \frac{100}{w_{100} - w_{50}} \quad (16)$$

Table 4. Linear stiffness values of edge joints obtained by numerical simulation.

n	2	3	5
$K_{l,sim}$	51.8	66.0	84.3
$K_{l,fit}$	22.6	28.6	33.9

According to equation.13, the total linear stiffness is the edge joint linear stiffness when the corner joint stiffness is infinite:

$$\lim_{k_{cl}\to\infty} \frac{1}{K_l} = \frac{1}{k_{sl}} \quad (17)$$

3.2.1. Setting Corner Joints to Semi-Rigid.

The steps to modify the corner joints to be semi-rigid are as follows:

1. Removing coupling constraints at the corner joint (Figure 10) and replace it with a semi-rigid joint rotating in the direction of the Z-axis (spring constraint);
2. The corner joint rotational stiffness $k_{ca}(\times 10^4 N \cdot mm/Rad)$ was assigned different values and substituted into the numerical simulation model to obtain the values of total linear stiffness $K_{l,sim}$ considering the semi-rigid corner joints (Table 5).

Comparing the values of $K_{l,sim}$ corresponding to Table 4 and Table 5, the effect of the semi-rigidity of the corner joints on the total linear stiffness of the structure can be seen.

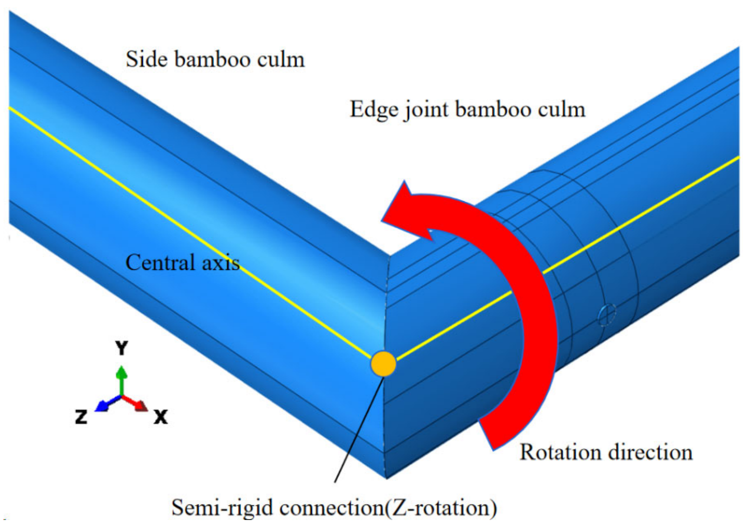

Figure 10. Semi-rigid corner joints.

By equation.11, the value assigned to k_{ca} above is converted to k_{cl}, and substituting into equation.13 can calculate the total linear stiffness $K_{l,equ}$ (consider the semi-rigidity of corner joints, Table 5), where k_{sl} is obtained from equation.17 ($K_{l,sim}$ in Table 4). Plotting the data in Table 5 as

Preprints.org (www.preprints.org) | NOT PEER-REVIEWED | Posted: 7 March 2024 doi:10.20944/preprints202403.0387.v1

Figure 11, the numerical simulation fits very well with the calculated values of equation.13, proving the feasibility and accuracy of replacing numerical simulation with equation.13.

Table 5. Linear stiffness values of edge joints obtained by numerical simulation.

	n=2			n=3			n=5	
k_{ca}	$K_{l,sim}$	$K_{l,equ}$	k_{ca}	$K_{l,sim}$	$K_{l,equ}$	k_{ca}	$K_{l,sim}$	$K_{l,equ}$
100	15.6	15.8	100	16.7	16.9	100	17.7	17.9
200	24.0	24.2	200	26.7	26.9	200	29.3	29.5
300	29.3	29.4	300	33.4	33.5	300	37.5	37.6
400	32.9	33.0	400	38.1	38.2	400	43.5	43.7

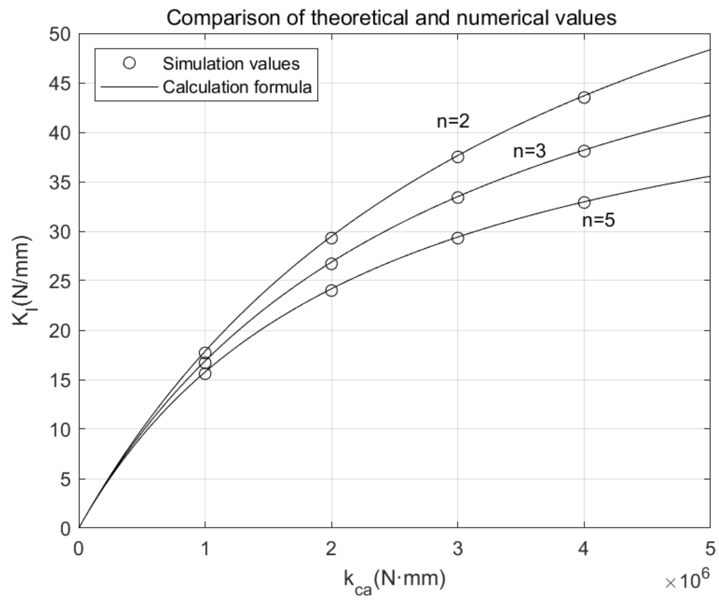

Figure 11. Comparison of theoretical and numerical values.

The values of linear stiffness k_{cl} for the considered semi-rigid corner joints can be obtained by bringing the first and second rows of Table 4 into equation.13 as k_{sl} and K_l, respectively. the value of k_{cl} after substituting into equation.11 is transformed into the value of k_{ca} as shown in Table 6. This value is the average rotational stiffness of the four corner joints connecting the edge joints in Figure 7, not the rotational stiffness of the corner joints in a specific certain position.

Table 6. Linear stiffness values of edge joints obtained by numerical simulation.

n	2	3	5
$k_{ca}(\times 10^4 N \cdot mm/Rad)$	176.8	222.6	250.1

3.3. Semi-Rigid Edge Joint

To analyze the effect of positions on the stiffness of the edge joints when the number of bolts is the same, s is defined as the distance from the outermost bolt to the axis of the side bamboo culm (Defined as "side distance", Figure 12), and $k_{sl}(s)$ is the linear stiffness of the edge joint as a function of s, the bolts arranged at equal distances. Through the numerical simulation method established in this paper, the k_{sl} corresponding to different values of s can be obtained, as shown in Table 7. The linear regression equations of k_{sl} and s are established:

$$k_{sl}(s) = As + B \tag{18}$$

where: A and B are coefficients to be determined.

Preprints.org (www.preprints.org) | NOT PEER-REVIEWED | Posted: 7 March 2024 doi:10.20944/preprints202403.0387.v1

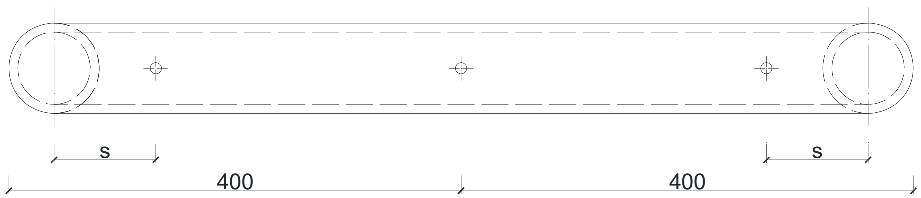

Figure 12. Side distance s.

Table 7. Linear stiffness values of edge joints obtained by numerical simulation.

n	2			3			5		
$s(mm)$	90	180	270	90	180	270	90	180	270
$k_{sl}(N/mm)$	51.8	42.4	36.3	66.0	54.0	45.3	84.3	67.8	56.0

Matlab is used to linearly fit the (s, k_{sl}) points of Table 7 according to equation.18, the $k_{sl} - s$ relationship can be obtained for different numbers of bolts, see Figure 13. The stiffness values calculated from the fitted relationship equation have an error of less than 3% compared to the stiffness values obtained from the numerical simulation, which indicates that the regression effect is good. It is also found that under the condition of the same number of bolts, k_{sl} increases linearly with the decrease of s, which indicates that the outer bolt closer to the corner joint is more beneficial for stiffness improvement.

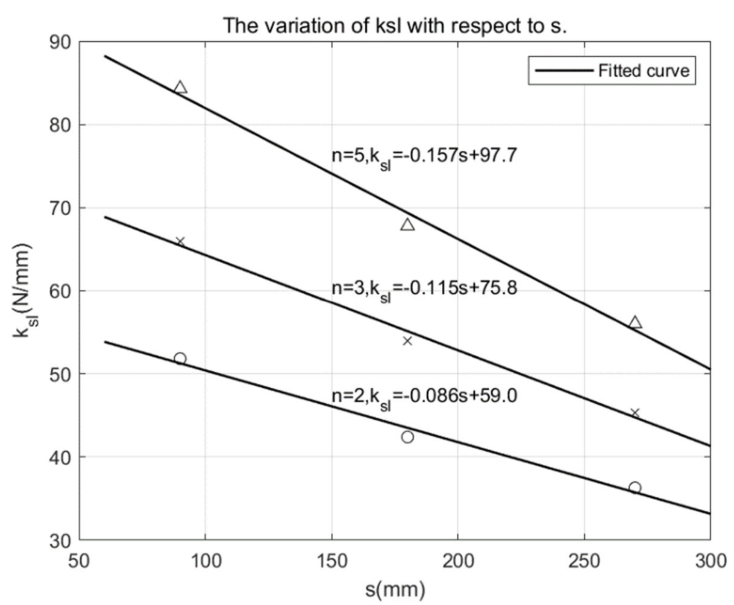

Figure 13. K-s relationship for different number of bolts.

By substituting the fitting equation in Figure 13 and b=420mm into equation.10, the calculation formula for the rotational stiffness of the edge joint can be obtained when the diameter of the bolts in the edge joint is set to 10mm.

$$k_{sa}(s) = \begin{cases} -3797.5s + 260.2 \times 10^4, n = 2 \\ -5071.5s + 334.3 \times 10^4, n = 3 \\ -6933.5s + 430.7 \times 10^4, n = 5 \end{cases} \tag{19}$$

From equation.3 and 4, the rotational stiffness of the joint is the relative angle of rotation produced under the action of unit bending moment, which is a property of the joint itself. Therefore, equation.19 is a general formula for the rotational stiffness of the corner joint when the diameter of the bolts of the edge joint are 10 mm. Similarly, the rotational stiffness values k_{ca} in Table 6 are generic values for corner joints in a specific configuration (using 4 screws combined with wooden plugs). These values and formulas derived from experimental data, numerical simulations and

Preprints.org (www.preprints.org) | NOT PEER-REVIEWED | Posted: 7 March 2024 doi:10.20944/preprints202403.0387.v1

theoretical derivations provide a basis for the setting of joint semi-stiffness in structural finite element analyses.

4. Finite Element Analysis of Structures and Design Methods for Components

The finite element analysis method of the structure is to model the components according to the axes, and since the calculation formulas and parameters obtained in Chapter 3 of this paper are based on solid modelling, a practical method for the finite element analysis and component design of the bamboo culm and frame-unit bamboo culm structure will be presented in this chapter. The equivalent joint forces and joint deformations in the structure are first analyzed according to the computational model in Figure 7, and then the internal forces of the bamboo culm and bolts are calculated in combination with the computational model, then the allowable stresses and deformations of each component are verified.

Taking the model shown in Figure 4 as an example, the material, size and number of bolts of the two bamboo culm frame units are the same as those of the S5test in the test, i.e., : the outer diameter D of the bamboo culm is 80mm, the thickness of the bamboo wall t is 8mm, and the size of the outer frame of the bamboo culm frame: L×H=800mm×500mm (axial figure: a=720mm, b=420mm). The edge joint is connected by 5 bolts with d=10mm, the side distance s is 90mm, and the rest of the bolts are arranged in equal distance from each other. The corner joints are connected by 4 screws and wooden plugs. The support bamboo culm is used as the simply supported side. The top of the edge joint bamboo culm is subjected to a uniform load, and the total force F is consistent with the experimental value in Figure 6, which is taken as 413N.

4.1. Structural Finite Element Analysis Methods

4.1.1. Structural Modelling

The equivalent computational model of each member is shown in Figure 14:

1. Select the axis of each bamboo culm as the position of the equivalent members;
2. An equivalent bolt is set at the midpoint of the edge joint bamboo culm, and the connection between the equivalent bolt and the edge joint bamboo culm is a rigid connection. The middle position of the equivalent bolt is disconnected, and the disconnection is set as a semi-rigid connection;
3. All corner joints are set to semi-rigid connections;
4. The two ends of the support bamboo culms are set as hinged.

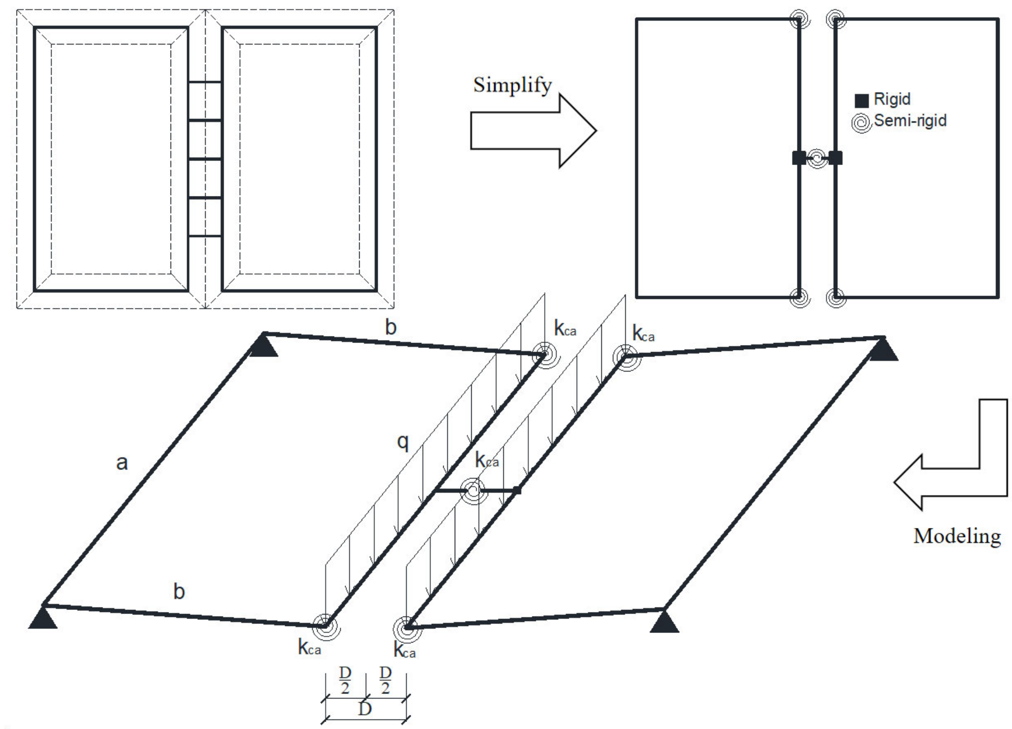

Figure 14. Equivalent solid model to beam model.

4.1.2. Parameter Settings

Since the corner and edge joint stiffnesses studied in this paper already include the deformation of the material itself, to avoid repeated calculations, the members should be set as rigid bodies during the finite element analysis of the structure, i.e., : the stiffness and elastic modulus of various materials are set to infinity. The semi-rigid joints are set as follows:

From Table 6, the rotational stiffness of the corner joints:

$$k_{ca} = 250.1 \times 10^4 N \cdot mm/Rad$$

From equation.19, the edge joint rotational stiffness:

$$k_{sa} = -6933.5 \times 90 + 430.7 \times 10^4 = 368.3 \times 10^4 N \cdot mm/Rad$$

Taking the test data at n=5 in Figure 6 when the load is 413 N, the uniform load on the edge joint bamboo culms:

$$q = \frac{F}{2(L-2D)} = \frac{413}{2 \times (800 - 2 \times 80)} = 0.32 N/mm$$

4.1.3. Calculation Result

The maximum deflection obtained by using Abaqus is 12.2 mm, while the measured value of the test in Figure 6 is 13.0 mm, which indicates that the calculation method in this paper has a good calculation accuracy.

4.2. Design Methods for Components

4.2.1. Internal Force Distribution

The software calculates the maximum bending moment on the equivalent edge joint bolt to be $8.68 \times 10^4 N \cdot mm$, which is the value of the combined cross sectional internal force in the mid-span of each bolt in the actual structure, so this equivalent joint force needs to be assigned to each bolt.

Preprints.org (www.preprints.org) | NOT PEER-REVIEWED | Posted: 7 March 2024 doi:10.20944/preprints202403.0387.v1

The bending moment at the equivalent edge joint was distributed to each bolt according to the distribution ratio coefficients in Table 3, and the values of bending moments on the five bolts were obtained as 2.24, 1.47, 1.27, 1.47, 2.24 ($\times 10^4 N \cdot mm$), respectively. Substituting these values into the torque calculation sketch in Figure 15a gives the torque on each section of the bamboo culm at the edge joints (Figure 15b).

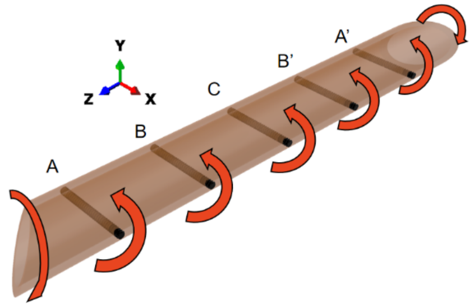

(a). Simplified diagram of torque calculation of bamboo culm with edge joints.

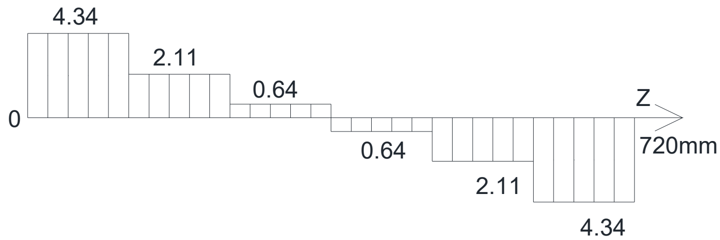

(b). Torque diagram for edge joint bamboo culm.

Figure 15. Torque calculation of edge joint bamboo culm.

4.2.2. Strength Calculation of Components

Figure 16 shows the force sketch of the bolt in bending, due to the thin wall of the bamboo pipe, the constraint of the bamboo pipe wall on the bolt can be considered as simple support, force between the outermost bolt and the walls of the bamboo tube:

$$0.5P = \frac{M}{D} = \frac{2.24 \times 10^4}{80} = 280\ N$$

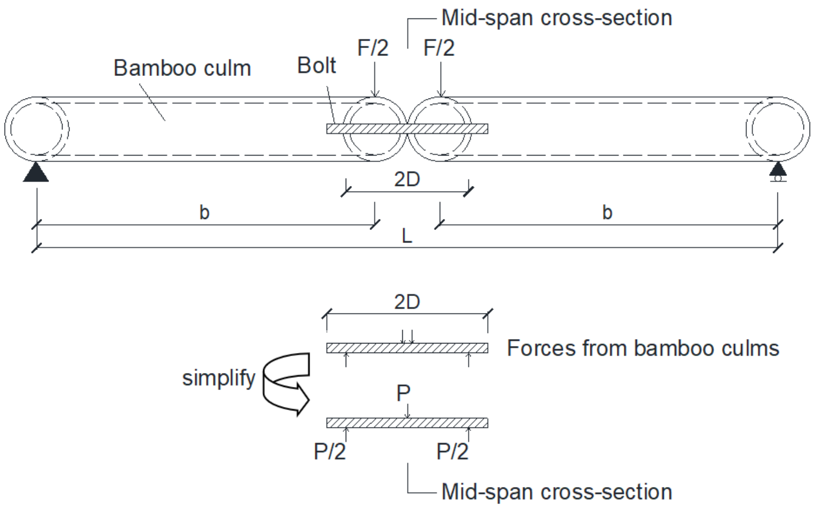

Figure 16. Bolt calculation diagram.

 doi:10.20944/preprints202403.0387.v1

Calculate the bearing compression stress at the location of the bamboo culm hole wall:

$$\sigma_{xc} = \frac{0.5P}{dt} = \frac{280}{10 \times 8} = 3.5\ MPa < 40.2MPa$$

Calculate the bending strength of the outermost bolt.:

$$\sigma_{max} = \frac{M}{W} = \frac{2.24 \times 10^4}{\frac{\pi \times 10^3}{32}} = 228.2MPa < 235MPa$$

Calculate the torsional strength of the bamboo culm by taking the maximum torque of the bamboo culm:

$$\tau_{max} = \frac{T}{W_p} = \frac{4.34 \times 10^4}{\frac{\pi}{16 \times 80}(80^4 - 72^4)} = 1.3MPa < 25MPa$$

5. Conclusions

1. The results of experimental and numerical simulation analyses show that the total flexural stiffness of the combined member is positively correlated with the number of bolts at the edge joint, but the efficiency of the increase decreases with the increase in the number of bolts. With the same number of bolts, it is more beneficial for the outer bolts to be close to the corner joints on that side to increase the flexural linear stiffness of the edge joint.
2. The calculation model of the frame-unit bamboo culm members considering the semi-rigidity of the joint is proposed, and the conversion formula between the linear stiffness of the corner and the edge joints and their rotational stiffness is deduced through the geometric relationship between the displacement and the rotation. The series and parallel relationship between corner joints and edge joints in the structure is established, and the general relationship equation between the total stiffness of the frame-unit structure and the stiffness of corner joints and edge joints is derived.
3. A numerical simulation method for semi-rigid joint of frame-unit bamboo culm structure is proposed. Based on the general relationship of stiffness, the corner joints are first set as completely rigid. By establishing numerical simulation, the semi-rigid rotational stiffness values, and calculation formulas of edge joints under different bolt quantity can be obtained. Then, by substituting the edge joint stiffness values obtained from numerical simulation and the total stiffness values obtained from experiments into the general relationship formula, the average semi-rigid rotational stiffness value of corner joints can be obtained. When the corner and edge joints are constructed in other forms, the method of combining test and numerical simulation proposed in this paper can also be used to obtain the corresponding rotational stiffness values and the calculation formula.
4. A finite element analysis method based on semi-rigid joints for frame-unit bamboo culm structure was proposed, calculated results are close to the test values, internal force sketches and calculations for bamboo culms and joints are presented, which can be used for internal force analysis and design of frame-unit prefabricated bamboo culm lattice structures.

Author Contributions: Conceptualization, Wang, G.J. and Zhuo, X.; methodology, Wang, G.J. and Zhuo, X.; software, Zhang, S.B.; validation, Wu, J. and Zhang, S.B.; experiment, Wu, J. and Zhang, S.B.; formal analysis, Wang, G.J.; resources, Wu, J. and Zhang, S.B.; data curation, Wu, J.; writing—original draft preparation, Wang, G.J.; writing—review and editing, Wang, G.J. and Zhuo, X.; supervision, Zhuo, X.; project administration, Zhuo, X.; funding acquisition, Zhuo, X. All authors have read and agreed to the published version of the manuscript.

Funding: This research was funded by the National Key Research and Development Program, Grant No. 2017YFC0703500.

Data Availability Statement: Data will be made available on request.

Conflicts of Interest: The authors declare no conflicts of interest.

References

 doi:10.20944/preprints202403.0387.v1

1. Lorenzo R.; Mimendi L. Digitisation of bamboo culms for structural applications. *Build Eng*, **2020**, 29, Article 101193. https://doi.org/10.1016/j.jobe.2020.101193.
2. E. Zea Escamilla; G. Habert. Environmental impacts of bamboo-based construction materials representing global production diversity. *Journal of Cleaner Production*, **2014**, 69: 117-127. https://doi.org/10.1016/j.jclepro.2014.01.067.
3. Anokye R; Bakar SE; Ratnansingam J; Awang BK. Bamboo properties and suitability as a replacement for wood. *Pertanika J Sch Res Rev*, **2016,** 2(1): 63–79. DOI: 10.13140/RG.2.1.1939.3048.
4. Chung, K.F.; Yu, W. K.; Mechanical properties of structural bamboo for bamboo scaffoldings. *Eng. Struct*, **2002**, *24: 429-442. DOI: 10.1016/S0141-0296(01)00110-9.*
5. Adier, M.F.V.; Sevilla, M.E.P.; Valerio, D.N.R.; Ongpeng, J.M.C. Bamboo as Sustainable Building Materials: A Systematic Review of Properties, Treatment Methods, and Standards. *Buildings*, **2023**, 13: 2449. https://doi.org/10.3390/buildings13102449.
6. Li, R. R.; He, C. J.; Peng Bo.; Wang, C. G. Differences in fiber morphology and partial physical properties in different parts of Phyllostachys edulis. *Journal of Zhejiang A&F University*, **2021**, 38(4): 854-860. DOI: 10.11833/j.issn.2095-0756.20200649. (in Chinese)
7. Hong, C. K.; Li, H. T.; R. Lorenzo; Wu, G.; I. Corbi; O. Corbi; Xiong, Z. H.; Yang, D.; Zhang, H. Z. Review on connections for original bamboo structures. *Journal of Renewable Materials*, **2019**, 7(8): 713–730. https://doi.org/10.32604/jrm.2019.07647.
8. Dai, P. Q.; Luo, Z. Y.; He, M. J. Structural design and analysis for shanghai expo special project DuC. *Structural Engineers*, **2011**, 27(4): 6—11. DOI:10.15935/j.cnki.jggcs.2011.04.011. (in Chinese)
9. Huang, T.; Zhuo, X. Experimental Study on the Bending Properties of Grouting Butt Joints Reinforced by Steel Plate Embedded in Bamboo Tube. *Journal of Renewable Materials*, **2022**, 10(4): 993–1005. DOI: 10.32604/jrm.2022.017373.
10. R. Moran; J.J. García. Bamboo joints with steel clamps capable of transmitting moment. *Construct Build Mater*, **2019**, *216: 249-260. https://doi.org/10.1016/j.conbuildmat.2019.05.025.*
11. B. Lefevre; R. West; P. O'Reilly; D. Taylor. A new method for joining bamboo culms. *Eng. Struct*, **2019**, 190: 1-8. DOI: 10.1016/j.engstruct.2019.04.003.
12. Minke G. Building with Bamboo. **2012**. Switzerland: Birkhäuser basel. *47-66.*
13. Liu, K. W.; Xu, Q. F.; Wang, G.; Chen, F. M.; Leng, Y. B.; Yang, J.; K. A. Harries. Contemporary Bamboo Architecture in China. **2022.** Beijing:TsingHua University press. *31-55.*
14. Zhuo, X.; Dong, S. L. Bamboo tube bundle spatial lattice structure system and construction technology. *Spatial Structure*, **2021**, 27(1): 3–8. DOI: 10.13849/j.issn.1006-6578.2021.01.003. (in Chinese)
15. Zhuo, X.; Dong, S. L. Frame-unit prefabricated bamboo culm lattice structure system and engineering practices. *Journal of building structures*, **2024**, *45(3): 43-51. https://doi.org/10.14006/j.jzjgxb.2023.0063.* (in Chinese)
16. Zhu, C. M.; Zhang, W. P. Structural Mechanics (volume 2). **2016**. Beijing: Higher Education Press. *51-54.* (in Chinese)
17. J. García, C. Rangel, K. Ghavami. Experiments with rings to determine the anisotropic elastic constants of bamboo. *Constr. Build. Mater*. **2010**. 31: 52-57. https://doi.org/10.1016/j.conbuildmat.2011.12.089.
18. Zhang, X. X.; Yu, Z. X.; Yu, Y.; Wang, H. K.; Li, J. H. Axial compressive behavior of Moso Bamboo and its components with respect to fiber-reinforced composite structure, *J. For. Res*. **2019**. 30(6): 2371–2377. https://doi.org/10.1007/s11676-018-0780-9.
19. Walter Liese; Michael Köhl. Bamboo The Plant and its Use. **2015.** Switzerland: Springer International Publishing. *251-253.*
20. Peng, H., Zhuo, X. Research on Mechanical Behavior of the Screwed Connection at the End of Bamboo Strip. Zhejiang University, Hangzhou, Zhejiang Province. **2022**. DOI: 10.27461/d.cnki.gzjdx.2022.001345. (in Chinese)